SPECFORMER: SPECTRAL GRAPH NEURAL NETWORKS MEET TRANSFORMERS

Anonymous authors
Paper under double-blind review

ABSTRACT

Spectral graph neural networks learn graph representations via spectral-domain graph convolutions. However, most existing spectral graph filters are scalar-to-scalar functions, i.e., mapping a single eigenvalue to a single filtered value, thus ignoring the global pattern of the spectrum. Furthermore, these filters are often constructed based on some fixed-order polynomials, which have limited expressiveness and flexibility. To tackle these issues, we introduce Specformer, which effectively encodes the set of all eigenvalues and performs self-attention in the spectral domain, leading to a learnable set-to-set spectral filter. We also design a decoder with learnable bases to enable non-local graph convolution. Importantly, Specformer is equivariant to permutation. By stacking multiple Specformer layers, one can build a powerful spectral graph neural network. On synthetic datasets, we show that our Specformer can better recover ground-truth spectral filters than other spectral GNNs. Extensive experiments of both node-level and graph-level tasks on real-world graph datasets show that our Specformer outperforms state-of-the-art GNNs and learns meaningful spectrum patterns.

1 INTRODUCTION

Graph neural networks (GNNs), firstly proposed in (Scarselli et al., 2008), become increasingly popular in the field of machine learning due to their empirical successes. Depending on how the graph signals (or features) are leveraged, GNNs can be roughly categorized into two classes, namely spatial GNNs and spectral GNNs. Spatial GNNs often adopt a message passing framework (Gilmer et al., 2017; Battaglia et al., 2018) which propagates local information on graphs to directly learn useful representations in the spatial domain. Spectral GNNs (Bruna et al., 2013; Defferrard et al., 2016) instead perform graph convolutions via spectral filters (*i.e.*, filters applied to the spectrum of the graph Laplacian), which can learn to capture non-local dependencies in spatial graph signals. Although spatial GNNs have achieved impressive performances in many domains, spectral GNNs are somewhat underexplored.

There are a few reasons why spectral GNNs have not been able to catch up. First, most existing spectral filters are essentially scalar-to-scalar functions. In particular, they can only take a single eigenvalue as input and output a filtered value while ignoring the rich information embedded in the spectrum, *i.e.*, the set of eigenvalues. For example, we know from the spectral graph theory that the algebraic multiplicity of the eigenvalue 0 tells us the number of connected components in the graph. However, such information can not be captured by the scalar-to-scalar filters. Second, the spectral filters are often approximated via fixed-order (or truncated) orthonormal bases (*e.g.*, Chebyshev polynomials (Defferrard et al., 2016; He et al., 2022) and graph Wavelets (Hammond et al., 2011; Xu et al., 2019)) in order to avoid the costly spectral decomposition of the graph Laplacian. Although the orthonormality is a nice property, this truncated approximation is less expressive and may severely limit the graph representation learning.

Therefore, in order to improve spectral GNNs, it is natural to ask: *how can we build expressive spectral filters that can effectively leverage the spectrum of graph Laplacian*? To answer this question, we first note that eigenvalues of graph Laplacian represent the frequency, *i.e.*, total variation of the corresponding eigenvectors. The magnitudes of frequencies thus convey rich information. Moreover, the relative difference between two eigenvalues also reflects important frequency information, *e.g.*, the spectral gap. To capture both magnitudes of frequency and relative frequency, we propose

a Transformer (Vaswani et al., 2017b) based set-to-set spectral filter, termed *Specformer*. Our Specformer first encodes the range of eigenvalues via positional embedding and then exploits the self-attention mechanism to learn relative information from the set of eigenvalues. Relying on the learned representations of eigenvalues, we also design a decoder with a bank of learnable bases. Finally, by combining these bases, Specformer can construct a permutation-equivariant and non-local graph convolution. In summary, our contributions are as follows:

- We propose a novel Transformer-based set-to-set spectral filter along with learnable bases, called Specformer, which effectively captures both magnitudes and relative dependencies of all eigenvalues of the graph Laplacian.
- We show that Specformer is permutation equivariant and can perform non-local graph convolutions, which is non-trivial to achieve in many spatial GNNs.
- Experiments on synthetic datasets show that Specformer better learns to recover the given spectral filters than other Spectral GNNs.
- Extensive experiments on various node-level and graph-level benchmarks demonstrate that Specformer outperforms state-of-the-arts GNNs and learns meaningful spectrum patterns.

2 Related Work

Existing GNNs can be roughly divided into two categories: spatial and spectral GNNs.

Spatial GNNs. Spatial-based GNNs like GCN (Kipf & Welling, 2017), GAT (Velickovic et al., 2018) and MPNN (Gilmer et al., 2017) leverage message passing to aggregate local information from neighborhood in the vertex domain. By stacking multiple layers, spatial GNNs can learn long-range information but suffers from over-smoothing Oono & Suzuki (2020) and over-squashing Topping et al. (2022). Therefore, how to balance local and global information is an important topic in spatial GNNs. We refer readers to (Wu et al., 2021; Zhou et al., 2020) for a more detailed survey.

Spectral GNNs. Spectral GNNs (Wu et al., 2019; Zhu et al., 2021; Bo et al., 2021; Chang et al., 2021; Yang et al., 2022) leverage the spectrum of graph Laplacian to perform convolutions in the spectral domain. It has shown great potential in graph-related tasks (Ortega et al., 2018; Dong et al., 2020). Most spectral GNNs focus on the design of spectral filters. Polynomial based GNNs are a popular subclass of spectral GNNs, which take advantage of the diagonalization of symmetric matrices to avoid direct spectral decomposition and guarantee localization. They leverage different kinds of polynomials to approximate arbitrary filters, including Monomial (Chien et al., 2021), Chebyshev (Defferrard et al., 2016; He et al., 2022), Bernstein (He et al., 2021), and Jacobi (Wang & Zhang, 2022). However, all the polynomial filters are scalar-to-scalar functions, and the bases are pre-defined, which greatly limits the expressiveness and learning ability. Another subclass of spectral GNN requires spectral decomposition, such as SpectralCNN (Estrach et al., 2014) and LanczosNet (Liao et al., 2019). They parameterize the spectral filters by neural networks, thus getting rid of the truncated polynomials based approximation. However, the spectral filters are still limited as they do not capture the dependencies among multiple eigenvalues.

Graph Transformer. Transformers and GNNs are closely relevant since the attention weights of Transformer can be seen as a weighted adjacency matrix of a fully connected graph. Graph Transformer is the combination of both and is first implemented by Dwivedi & Bresson (2020). Graphormer (Ying et al., 2022) further adds structural encoding and achieves state-of-the-art performances on some graph-level tasks. SAN (Kreuzer et al., 2021) and GPS (Rampásek et al., 2022) design powerful positional and structural embeddings for graph Transformers to improve its expressive power. Graph Transformers still belong to spatial GNNs, despite the high-cost self-attention is non-local.

3 Background

In this section, we introduce some preliminaries of graph signal processing (GSP) (Ortega et al., 2018) and Transformer (Vaswani et al., 2017a).

Preliminary. Assume that we have a graph $\mathcal{G} = (\mathcal{V}, \mathcal{E})$, where $\mathcal{V}$ denotes the node set with $|\mathcal{V}| = n$ and $\mathcal{E}$ is the edge set. The corresponding adjacency matrix $\boldsymbol{A} \in \{0,1\}^{n\times n}$, where $A_{ij} = 1$ if there is an edge between nodes i and j, and $A_{ij} = 0$ otherwise. The normalized graph Laplacian matrix is defined as $\boldsymbol{L} = \boldsymbol{I}_n - \boldsymbol{D}^{-1/2}\boldsymbol{A}\boldsymbol{D}^{-1/2}$, where $\boldsymbol{I}_n$ is the $n \times n$ identity matrix and $\boldsymbol{D}$ is the diagonal degree matrix with diagonal entries $D_{ii} = \sum_j A_{ij}$ for all $i \in \mathcal{V}$ and off-diagonal entries $D_{ij} = 0$ for $i \neq j$. We assume $\mathcal{G}$ is symmetric. Hence, $\boldsymbol{L}$ is a real symmetric matrix, whose spectral decomposition can be written as $\boldsymbol{L} = \boldsymbol{U}\boldsymbol{\Lambda}\boldsymbol{U}^\top$, where the columns of $\boldsymbol{U}$ are the eigenvectors and $\boldsymbol{\Lambda} = \text{diag}([\lambda_1, \lambda_2, \ldots, \lambda_n])$ are the corresponding eigenvalues ranged in $[0, 2]$.

Graph Signal Processing (GSP). Spectral GNNs rely on several important concepts from GSP, namely, spectral filtering, graph Fourier transform and its inverse. The graph Fourier transform is written as $\hat{\boldsymbol{x}} = \boldsymbol{U}^\top\boldsymbol{x}$, where $\boldsymbol{x} \in \mathbb{R}^{n\times 1}$ is a graph signal and $\hat{\boldsymbol{x}} \in \mathbb{R}^{n\times 1}$ represents the Fourier coefficients. Then a spectral filter G_θ is used to scale $\hat{\boldsymbol{x}}$. Finally, the inverse graph Fourier transform is applied to yield the filtered signal in spatial domain $\tilde{\boldsymbol{x}} = \boldsymbol{U}G_\theta\hat{\boldsymbol{x}}$. The key task in GSP is to design a powerful spectral filter G_θ so that we can exploit the useful frequency information.

Transformer. Transformer is a powerful deep learning model, which is widely used in natural language processing (Devlin et al., 2019), vision (Dosovitskiy et al., 2021), and graphs (Ying et al., 2022; Rampásek et al., 2022). Each Transformer layer consists of two components: a multi-head self-attention (MHA) module and a token-wise feed-forward network (FFN). Given the input representations $\boldsymbol{H} = [\boldsymbol{h}_1^\top, \ldots, \boldsymbol{h}_n^\top] \in \mathbb{R}^{n\times d}$, where d is the hidden dimension, MHA first projects $\boldsymbol{H}$ into query, key and value through three matrices ($\boldsymbol{W}^Q$, $\boldsymbol{W}^K$ and $\boldsymbol{W}^V$) to calculate attentions. And FFN is then used to add transformation. The model can be written as follows. For simplicity, we omit the bias and the description of multi-head attention.

$$\begin{aligned} \text{Attention}(\boldsymbol{Q}, \boldsymbol{K}, \boldsymbol{V}) &= \text{Softmax}(\frac{\boldsymbol{Q}\boldsymbol{K}^\top}{\sqrt{d_q}})\boldsymbol{V}, \\ \boldsymbol{Q} = \boldsymbol{H}\boldsymbol{W}^Q,\ \boldsymbol{K} &= \boldsymbol{H}\boldsymbol{W}^K,\ \boldsymbol{V} = \boldsymbol{H}\boldsymbol{W}^V. \end{aligned} \tag{1}$$

4 SPECFORMER

In this section, we introduce our proposed Specformer model. Fig. 1 illustrates the model architecture. We first explain how we vectorize the scalar eigenvalues through an encoding function and use Transformer to learn their dependency to yield useful representations. Then we turn to the decoder, which learns new eigenvalues from the representations and reconstructs the message passing matrix for graph convolution. Finally, we discuss the relationship between our Specformer and other methods, including MPNNs, polynomial GNNs, and graph Transformers.

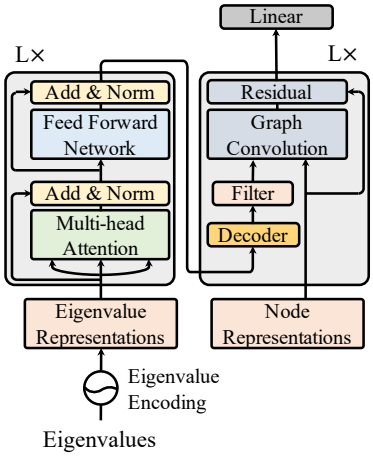

Figure 1: Illustration of the proposed Specformer.

4.1 EIGENVALUE ENCODING

We design a powerful set-to-set spectral filter using Transformer to learn both magnitudes and dependencies of the set of all eigenvalues. However, the expressiveness of self-attention will be restricted heavily if we directly use the scalar eigenvalues to calculate the attention maps. Therefore, it is important to find a suitable function, $\rho(\lambda) : \mathbb{R}^1 \to \mathbb{R}^d$, to map each eigenvalue from a scalar to a meaningful vector. We use an eigenvalue encoding function as follows.

$$\begin{aligned} \rho(\lambda, 2i) &= \sin(\epsilon\lambda/10000^{2i/d}), \\ \rho(\lambda, 2i+1) &= \cos(\epsilon\lambda/10000^{2i/d}), \end{aligned} \tag{2}$$

where i is the dimension of the representations and ϵ is a hyperparameter. The benefits of $\rho(\lambda)$ are three-fold. (1) It can capture the relative frequency shifts of eigenvalues and provides high-dimension

vector representations. (2) It has the wavelengths from 2π to $10000 \cdot 2\pi$, which forms a multi-scale representation for eigenvalues. (3) It can control the influence of λ by adjusting the value of ϵ.

The choice of ϵ is crucial because we find that only the first few dimensions of $\rho(\lambda)$ can distinguish different eigenvalues if we simply set $\epsilon = 1$. The reason is that eigenvalues lie in the range $[0, 2]$, and the value of $\lambda/10000^{2i/d}$ will change slightly when i becomes larger. Therefore, it is important to assign a large value of ϵ to enlarge the influence of λ. Experiments can be seen in Appendix C.1.

Notably, although the eigenvalue encoding (EE) is similar to the positional encoding (PE) of Transformer, they act quite differently. PE describes the information of discrete positions in the spatial domain. While EE represents the information of continuous eigenvalues in the spectral domain. Applying PE to the spatial positions (*i.e.*, indices) of eigenvalues will destroy the permutation equivariance property, thereby impairing the learning ability.

The initial representations of eigenvalues are the concatenation of eigenvalues and their encodings, $\boldsymbol{Z} = [\lambda_1 \| \rho(\lambda_1), \cdots, \lambda_n \| \rho(\lambda_n)]^\top \in \mathbb{R}^{n \times (d+1)}$. Then a standard Transformer block is used to learn the dependency between eigenvalues. We first apply layer normalization (LN) on the representations before feeding them into other sub-layers, *i.e.*, MHA and FFN. This *pre-norm* trick has been used widely to improve the optimization of Transformer Ying et al. (2022):

$$\begin{aligned} \tilde{\boldsymbol{Z}} &= \text{MHA}(\text{LN}(\boldsymbol{Z})) + \boldsymbol{Z}, \\ \hat{\boldsymbol{Z}} &= \text{FFN}(\text{LN}(\tilde{\boldsymbol{Z}})) + \tilde{\boldsymbol{Z}}. \end{aligned} \tag{3}$$

After stacking multiple Transformer blocks, we obtain the expressive representations of the spectrum through the encoder.

4.2 Eigenvalue Decoding

Based on the representations returned by the encoder, the decoder can learn new eigenvalues for spectral filtering. Recent studies (Yang et al., 2022; Wang & Zhang, 2022) show that assigning each feature dimension a separate spectral filter improves the performance of GNNs. Motivated by this discovery, our decoder first decodes several bases. An MLP is then used to combine these bases to construct the final graph convolution.

Spectral filters. In general, the bases should learn to cover different information of the graph signal space as much as possible. For this purpose, we utilize the multi-head mechanism of self-attention because each head has its own self-attention pipeline. Specifically, the representations learned by each head will be fed into the decoder to perform spectral filtering to get the new eigenvalues.

$$\boldsymbol{Z}_m = \text{Attention}(\boldsymbol{Q}\boldsymbol{W}_m^Q, \boldsymbol{K}\boldsymbol{W}_m^K, \boldsymbol{V}\boldsymbol{W}_m^V), \ \boldsymbol{\lambda}_m = \phi(\boldsymbol{Z}_m \boldsymbol{W}_\lambda), \tag{4}$$

where $\boldsymbol{Z}_m$ denotes the representations learned by the m-th heads, and ϕ is the activation, e.g., ReLU or Tanh, which is optional. $\boldsymbol{\lambda}_m \in \mathbb{R}^{n \times 1}$ is the m-th eigenvalues after the spectral filtering.

Learnable bases. After get M filtered eigenvalues, we use an MLP: $\mathbb{R}^{M+1} \to \mathbb{R}^d$ to construct the learnable bases. We first reconstruct individual new bases and them combine them by concatenating and feed it to a MLP.

$$\boldsymbol{S}_m = \boldsymbol{U}\text{diag}(\boldsymbol{\lambda}_m)\boldsymbol{U}^\top, \ \hat{\boldsymbol{S}} = \text{MLP}([\boldsymbol{I}_n || \boldsymbol{S}_1 || \cdots || \boldsymbol{S}_M]), \tag{5}$$

where $\boldsymbol{S}_m \in \mathbb{R}^{n \times n}$ is the m-th new basis and $\hat{\boldsymbol{S}}$ is the combined version. Note that our bases here serve similar purpose as those polynomial bases in the literature. But the way they are combined is learned rather than following certain recursions as in Chebyshev polynomials.

We have three optional ways to leverage this design of new bases. (1) Shared filters and shared MLP. This model has the least parameters, where the basis $\hat{\boldsymbol{S}}$ is shared across all graph convolutional layers. (2) Shared filters and layer-specific MLP, which compromises between parameters and performance, *e.g.*, $\hat{\boldsymbol{S}}^{(l)} = \text{MLP}^{(l)}([\boldsymbol{I}_n || \boldsymbol{S}_1 || \cdots || \boldsymbol{S}_M])$ where l denotes the index of layer. (3) Layer-specific filters and layer-specific MLP. This model has the most parameters and each layer has its own encoder and decoder, *e.g.*, $\hat{\boldsymbol{S}}^{(l)} = \text{MLP}^{(l)}([\boldsymbol{I}_n || \boldsymbol{S}_1^{(l)} || \cdots || \boldsymbol{S}_M^{(l)}])$. We refer these three models as Specformer-Small, Specformer-Medium, and Specformer-Large.

4.3 GRAPH CONVOLUTION

Finally, we assign each feature dimension a separate graph matrix based on the learned basis $\hat{\boldsymbol{S}}$, which can be written as follows:

$$\hat{\boldsymbol{X}}_{:,i}^{(l-1)} = \hat{\boldsymbol{S}}_i \boldsymbol{X}_{:,i}^{(l-1)}, \ \boldsymbol{X}^{(l)} = \sigma\left(\hat{\boldsymbol{X}}^{(l-1)} \boldsymbol{W}_x\right) + \boldsymbol{X}^{(l-1)}, \tag{6}$$

where $\boldsymbol{X}^{(l)}$ is the node representations in the l-th layer, $\boldsymbol{W}_x$ is the transformation, and σ is the activation. The residual connection is an optional choice. By stacking multiple graph convolutional layers, Specformer can effectively learn node representations for downstream tasks.

4.4 KEY PROPERTIES COMPARED TO RELATED MODELS

Specformer *v.s.* Polynomial GNNs. Specformer replaces the fixed bases of polynomials, *e.g.*, $\lambda, \lambda^2, \cdots, \lambda^k$, with learnable bases, which has two major advantages: (1) Universality. Polynomial GNNs are the special cases of Specformer because the learnable bases can approximate any polynomials. (2) Flexibility. Polynomial GNNs are designed to learn a shared function for all eigenvalues whereas Specformer can learn eigenvalue-specific functions, thus being more flexible.

Specformer *v.s.* MPNNs. MPNNs aggregate the local information from neighborhood layer by layer. This localization capability enables MPNNs with high computional efficiency but weakens the global information. Specformer is inherently non-localized due to the use of dense eigenvectors. The learned basis $\boldsymbol{U}G_\theta\boldsymbol{U}^\top$ can be rewritten as $\theta_1\boldsymbol{u}_1\boldsymbol{u}_1^\top + \cdots + \theta_n\boldsymbol{u}_n\boldsymbol{u}_n^\top$. Because $\boldsymbol{u}_i$ is a dense vector, $\boldsymbol{u}_i\boldsymbol{u}_i^\top$ constructs a fully-connected space. With proper weights of G_θ, the graph can break the localization of MPNNs and capture global information.

Specformer *v.s.* Graph Transformers. Graph Transformers are also non-local because of the fully-connected node attention matrix. Graphormer Ying et al. (2022) has shown that Transformer can perform well on graph-level tasks. However, existing graph Transformers do not show competitiveness in the node-level tasks, *e.g.*, classification. Recent studies Wang et al. (2022); Shi et al. (2022) provide some evidence for this phenomenon. They show that Transformer is essentially a low-pass filter. Therefore, graph Transformers cannot handle the complex node label distribution, *e.g.*, homophilic and heterophilic. On the contrary, as we will see in the experiment section, Specformer can learn arbitrary bases for graph convolution and perform well on both node-level and graph-level tasks.

Permutation equivariant. We show that Specformer is permutation equivariant. First, due to the proposed eigenvalue encoding, the representations of eigenvalues are invariant to the changes in spatial locations, *e.g.*, node permutations. Besides, the self-attention module satisfies $(\boldsymbol{P}\boldsymbol{Z}\boldsymbol{P}^\top)(\boldsymbol{P}\boldsymbol{Z}\boldsymbol{P}^\top)^\top = \boldsymbol{P}(\boldsymbol{Z}\boldsymbol{Z}^\top)\boldsymbol{P}^\top$, where $\boldsymbol{P}$ is a permutation matrix. Finally, it is straightforward to show that graph convolution in Eq. (6) is permutation equivariant. Therefore, Specformer is permutation equivariant.

Complexity. The time complexity of Specformer has three parts: The transformer block of the encoder, graph reconstructions of the decoder, and the graph convolutional layers. Their corresponding complexities are $\mathcal{O}(n^2d+nd^2)$, $\mathcal{O}(Mn^2)$ and $\mathcal{O}(Lnd)$, respectively, where n is the number of nodes, d is the dimension of the representations, M is the number of spectral filters, and L is the number of graph convolutional layers. Therefore, the overall complexity is $\mathcal{O}(n^2(d+M)+nd(L+d))$, which is linear with the quadratic of nodes.

5 EXPERIMENTS

In this section, we conduct experiments on a synthetic dataset and a wide range of real-world graph datasets to verify the effectiveness of our Specformer.

5.1 LEARNING SPECTRAL FILTERS ON SYNTHETIC DATA

We first test whether our Specformer can learn the pre-defined spectral filters on synthetic data.

Table 1: Node regression results, mean of the sum of squared error & R^2 score, on synthetic data.

Model ($\sim$**2k param.**)	**Low-pass** $\exp(-10\lambda^2)$	**High-pass** $1-\exp(-10\lambda^2)$	**Band-pass** $\exp(-10(\lambda-1)^2)$	**Band-rejection** $1-\exp(-10(\lambda-1)^2)$	**Comb** $\lvert\sin(\pi\lambda)\rvert$
GCN	3.4799(.9872)	67.6635(.2364)	25.8755(.1148)	21.0747(.9438)	50.5120(.2977)
GAT	2.3574(.9905)	21.9618(.7529)	14.4326(.4823)	12.6384(.9652)	23.1813(.6957)
ChebyNet	0.8220(.9973)	0.7867(.9903)	2.2722(.9104)	2.5296(.9934)	4.0735(.9447)
GPR-GNN	0.4169(.9984)	0.0943(.9986)	3.5121(.8551)	3.7917(.9905)	4.6549(.9311)
BernNet	0.0314(.9999)	0.0113(.9999)	0.0411(.9984)	0.9313(.9973)	0.9982(.9868)
JacobiConv	0.0003(.9999)	0.0064(.9999)	0.0213(.9999)	0.0156(.9999)	0.2933(.9995)
Specformer	**0.0002(.9999)**	**0.0026(.9999)**	**0.0017(.9999)**	**0.0014(.9999)**	**0.0057(.9999)**

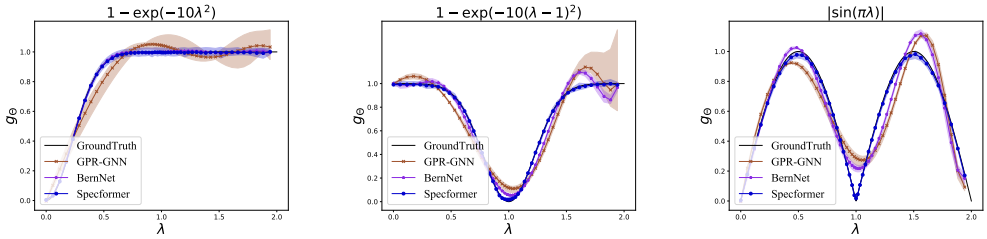

(a) High-pass (b) Band-rejection (c) Comb

Figure 2: Illustrations of filters learned by three polynomial GNNs and Specformer.

Dataset description. We take 50 images with a resolution of 100×100 from the Image Processing Toolbox [1]. Each image is processed as a 2D regular 4-neighborhood grid graph, and the values of pixels are the node features. Therefore, these images share the same adjacency matrix $\boldsymbol{A} \in \mathbb{R}^{10000\times 10000}$ and the m-th image has its graph signal $\boldsymbol{x}_m \in \mathbb{R}^{10000\times 1}$. Five predefined graph filters are used to generate ground truth graph signals. For example, if we use the low-pass filter with $G_\theta = \exp(-10\lambda^2)$, the filtered graph signal is calculated by $\tilde{\boldsymbol{x}}_m = U\text{diag}[\exp(-10\lambda_1^2), \ldots, \exp(-10\lambda_n^2)]U^\top \boldsymbol{x}_m$.

Setup. We choose six Spectral GNNs as baselines: GCN (Kipf & Welling, 2017), GAT (Velickovic et al., 2018), ChebyNet (Defferrard et al., 2016), GPR-GNN (Chien et al., 2021), BernNet (He et al., 2021), and JacobiConv (Wang & Zhang, 2022). Each method takes $\boldsymbol{A}$ and $\boldsymbol{x}_m$ as inputs, and tries to minimize the sum of squared error between the outputs $\hat{\boldsymbol{x}}_m$ and the pre-filtered graph signal $\tilde{\boldsymbol{x}}_m$. Following (He et al., 2021; Balcilar et al., 2021), we tune the number of hidden units to ensure that each method has nearly 2K trainable parameters. The polynomial order is set to 10 for ChebyNet, GPR-GNN, and BernNet. For our model, we use Specformer-Small with 16 hidden units and 1 head. In training, the maximum number of epochs is set to 2000, and the model will be stopped early if the loss does not descend 200 epochs. All regularization tricks are removed. The learning rate is set to 0.01 for all models. We use two metrics to evaluate each method: sum of squared error and R^2 score.

Results. The quantitative experiment results are shown in Table 1, from which we can see that Specformer achieves the best performance on all synthetic graphs. Especially, it has more improvements on challenging graphs, such as Band-rejection and Comb, which validate the effectiveness of Specformer in learning complex graph filters. In addition, we can see that GCN and GAT can only perform better on the homophilic graph, which reflects that only using low-frequency information is not enough. Polynomial-based GNNs, *i.e.*, ChebyNet, GPR-GNN, BernNet, and JacobiConv, have more stable performances. But their learning capacity is still weaker than Specformer. Figure 2 further validates our claims. We visualize the graph filters learned by GPR-GNN, BernNet, and Specformer. The horizontal axis presents the original eigenvalues, and the vertical axis indicates the corresponding new eigenvalues. For clarity, we uniformly downsample the eigenvalues at a ratio of 1:200 and only visualize three graphs because the situations of Low-pass and High-pass are similar. The same goes for Band-pass and Band-rejection. It can be seen that all methods can fit the easy filters well, *i.e.*, High-pass. However, the polynomial-based GNNs cannot learn the narrow bands in Band-rejection and Comb, *e.g.*, $\lambda \in [0.75, 1.25]$, which harms their performance. On the contrary, Specformer fits the ground truth precisely, reflecting the superior learning ability over polynomials.

[1] https://ww2.mathworks.cn/products/image.html

Table 2: Results on real-world node classification tasks. Mean accuracy (%) ± 95% confidence interval. * means re-implemented baselines; otherwise, the results are taken from the original papers.

	Param. on Photo	Heterophilic			Homophilic		
		Chameleon	**Squirrel**	**Actor**	**Cora**	**Citeseer**	**Photo**
Nodes	-	2,277	5,201	7,600	2,708	3,327	7,650
Edges	-	36,101	217,073	33,544	5,429	4,732	119,081
Features	-	2,325	2,089	932	1,433	3,703	745
Classes	-	5	5	5	7	6	8
Spatial-based GNNs							
GCN	48K	59.61±2.21	46.78±0.87	33.23±1.16	87.14±1.01	79.86±0.67	88.26±0.73
GAT	49K	63.13±1.93	44.49±0.88	33.93±2.47	88.03±0.79	80.52±0.71	90.94±0.68
H_2GCN	60K	57.11±1.58	36.42±1.89	35.86±1.03	86.92±1.37	77.07±1.64	93.02±0.91
GCNII	49K	63.44±0.85	41.96±1.02	36.89±0.95	88.46±0.82	79.97±0.65	89.94±0.31
Spectral-based GNNs							
LanczosNet*	50K	64.81±1.56	48.64±1.77	38.16±0.91	87.77±1.45	80.05±1.65	93.21±0.85
ChebyNet	48K	59.28±1.25	40.55±0.42	37.61±0.89	86.67±0.82	79.11±0.75	93.77±0.32
GPR-GNN	48K	67.28±1.09	50.15±1.92	39.92±0.67	88.57±0.69	80.12±0.83	93.85±0.28
BernNet	48K	68.29±1.58	51.35±0.73	41.79±1.01	88.52±0.95	80.09±0.79	93.63±0.35
ChebNetII	48K	71.37±1.01	57.72±0.59	41.75±1.07	88.71±0.93	80.53±0.79	-
JacobiConv	48K	74.20±1.03	57.38±1.25	41.17±0.64	**88.98±0.46**	80.78±0.79	95.43±0.23
Graph Transformers							
Transformer*	37K	46.39±1.97	31.90±3.16	39.95±1.64	71.83±1.68	70.55±1.20	90.05±1.50
Graphormer*	139K	54.49±3.11	36.96±1.75	38.45±1.38	67.71±0.78	73.30±1.21	85.20±4.12
Specformer	32K	**74.72±1.29**	**64.64±0.81**	**41.93±1.04**	88.57±1.01	**81.49±0.94**	**95.48±0.32**

5.2 Node Classification

Datasets. For the node classification task, we perform experiments on three homophilic datasets, *e.g.*, Cora, Citeser, and Amazon-Photo, and three heterophilic datasets, *e.g.*, Chameleon, Squirrel, and Actor. These datasets are commonly used in the previous literature (Chien et al., 2021; He et al., 2021; Wang & Zhang, 2022) to evaluate the learning ability of spectral GNNs.

Baselines and settings. We benchmark our model against a series of competitive baselines, including spatial-based GNNs (GCN, GAT, etc.), spectral-based GNNs (LanczosNet, ChebyNet, etc.), and graph Transformers. For all datasets, we use the full-supervised split, *i.e.*, 60% for training, 20% for validation, and 20% for testing, as suggested in (He et al., 2021). All methods run 10 times and report the mean accuracy with a 95% confidence interval. For polynomial GNNs, we set the order of polynomials $K = 10$. For other methods, we use a 2-layer module. To ensure all models have similar numbers of parameters, we set the hidden size $d = 64$ for spatial and spectral GNNs and $d = 32$ for graph Transformers and Specformer. The total parameters on Photo dataset are shown in Table 2.

Results. In Table 2, we can find that Specformer outperforms state-of-the-art baselines on 5 out of 6 datasets and achieves 12% relative improvement on the Squirrel dataset, which validates the superior learning ability of Specformer. In addition, the improvement is more pronounced on heterophilic datasets than on homophilic datasets. This is probably caused by the easier fitting of the low-pass filters in homophilic datasets. The same phenomenon is also observed in the synthetic graphs. An interesting observation is that the improvement on large graphs, *e.g.*, Actor and Photo, is less than that on small graphs. One possible reason is that the role of the self-attention mechanism is weakened, *i.e.*, the attention values become uniform due to a large number of tokens. We notice that Specformer has a slightly higher variance than the baselines. This is because we set a large dropout rate to prevent overfitting. Hyperparameters are listed in Appendix A.2.

5.3 Graph Classification and Regression

Datasets. We conduct experiments on three graph-level datasets with different scales. ZINC (Dwivedi et al., 2020) is a small subset of a large molecular dataset, which contains 12K graphs in total. MolHIV and MolPCBA are taken from the Open Graph Benchmark (OGB) datasets (Hu et al.,

Table 3: Results on graph-level datasets. ↓ means lower the better, and ↑ means higher the better.

Model	ZINC(↓)	MolHIV(↑)	MolPCBA(↑)
GCN	0.367 ± 0.011	0.7599 ± 0.0119	0.2424 ± 0.0034
GIN	0.526 ± 0.051	0.7707 ± 0.0149	0.2703 ± 0.0023
GatedGCN	0.090 ± 0.001	-	0.267 ± 0.002
CIN	0.079 ± 0.006	**0.8094 ± 0.0057**	-
GIN-AK+	0.080 ± 0.001	0.7961 ± 0.0119	0.2930 ± 0.0044
GSN	0.101 ± 0.010	0.7799 ± 0.0100	-
DGN	0.168 ± 0.003	0.7970 ± 0.0097	0.2885 ± 0.0030
PNA	0.188 ± 0.004	0.7905 ± 0.0132	0.2838 ± 0.0035
Spec-GN	0.070 ± 0.002	-	0.2965 ± 0.0028
SAN	0.139 ± 0.006	0.7785 ± 0.0025	0.2765 ± 0.0042
Graphormer	0.122 ± 0.006	-	-
GPS	0.070 ± 0.004	0.7880 ± 0.0101	0.2907 ± 0.0028
Specformer	**0.066 ± 0.003**	0.7889 ± 0.0124	**0.2972 ± 0.0023**

Table 4: Ablation studies on node-level and graph-level tasks.

Encoder		Decoder			Node-level		Graph-level
$\rho(\lambda)$	Attention	Small	Medium	Large	Squirrel (↑)	Citeseer (↑)	MolPCBA (↑)
			✓		33.05	80.57	0.2696
✓			✓		63.78	81.17	0.2933
✓	✓		✓		64.64	81.49	0.2970
✓	✓	✓			64.51	81.47	0.2912
✓	✓			✓	65.10	80.00	0.2972

2020). MolHIV is a medium dataset that has nearly 41K graphs. MolPCBA is the largest, containing 437K graphs. For all datasets, nodes represent the atoms, and edges indicate the bonds.

Baselines and Settings. We choose popular MPNNs (GCN, GIN, and GatedGNN), graph Transformers with positional or structural embedding (SAN, Graphormer, and GPS), and other state-of-the-art GNNs (CIN, GIN-AK+, etc.) as the baselines of graph-level tasks. For the ZINC dataset, we tune the hyperparameters of Specformer to ensure that the total parameters are around 500K.

Results. We apply Specformer-Small, Medium, and Large for ZINC, MolHIV, and MolPCBA, respectively. The results are shown in Table 3. It can be seen that Specformer outperforms the state-of-the-art models in ZINC and MolPCBA datasets, without using any hand-crafted features or pre-defined polynomials. This phenomenon proves that directly using neural networks to learn the graph spectrum is a possible way to construct powerful GNNs.

5.4 Ablation Studies

We perform ablation studies on two node-level datasets and one graph-level dataset to evaluate the effectiveness of each component. The results are shown in Table 4. The top three lines show the effect of the encoder, *i.e.*, eigenvalue encoding and self-attention. It can be seen that the encoding of eigenvalues is more important for Squirrel than Citeseer. The reason is that the spectrum of Squirrel is more difficult to learn. Therefore, the model needs encoding to learn better representations. The attention module consistently improves performance by capturing the dependency information.

The bottom three lines verify the performance of graph filters at different scales. We can see that in the easy task, *e.g.*, Citeseer, the Small and Medium models have similar performance, but the Large model causes serious overfitting. In the hard task, *e.g.*, Squirrel and MolPCBA, the Large model is slightly better than the Medium model but outperforms the Small model a lot, implying that adding the number of parameters can boost the performance. Overall, it is important to consider the difficulty of tasks when selecting models.

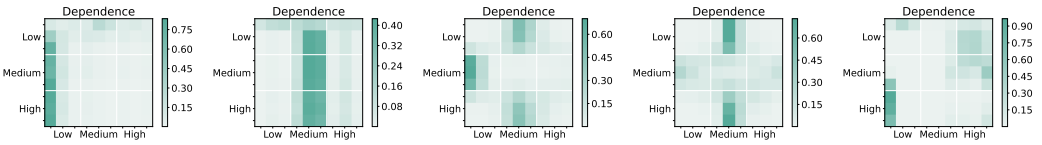

(a) Low-pass (b) High-pass (c) Band-pass (d) Band-rejection (e) Comb

Figure 3: The dependency of eigenvalues on synthetic graphs.

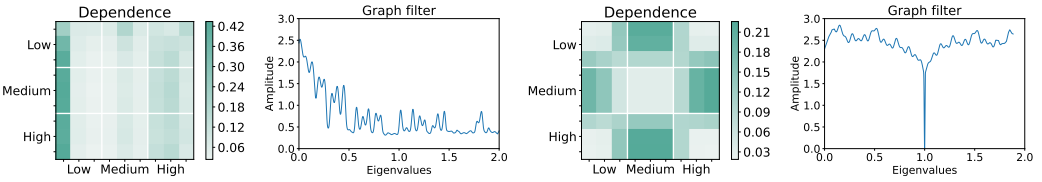

(a) Dependency of Citeseer (b) Filter of Citeseer (c) Dependency of Squirrel (d) Filter of Squirrel

Figure 4: The dependency and learned filters of heterophilic and homophilic datasets.

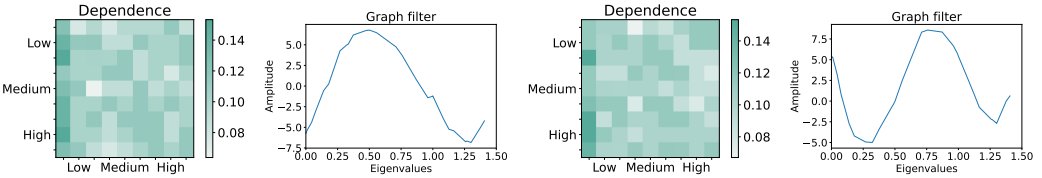

(a) dependency of $\hat{\boldsymbol{S}}_1$ (b) Filter of $\hat{\boldsymbol{S}}_1$ (c) dependency of $\hat{\boldsymbol{S}}_2$ (d) Filter of $\hat{\boldsymbol{S}}_2$

Figure 5: The dependency and basic filters of ZINC dataset.

5.5 Visualizations

We now investigate the dependency of eigenvalues and filters learned by Specformer. To make the dependency clearer, we first quantize the self-attention weight matrix by grouping the eigenvalues into three frequency bands: Low $\in [0, \frac{2}{3})$, Medium $\in [\frac{2}{3}, \frac{4}{3})$, and High $\in [\frac{4}{3}, 2]$. We then compute the quantized dependency. More details are given in Appendix B.2.

The results are shown in Figures 3, 4, and 5, from which we have some interesting observations. (1) Similar dependency patterns can be learned on different graphs. In low-pass filtering, *e.g.*, Citeseer and Low-pass, all frequency bands tend to use the low-frequency information. While, in the band-related filtering, *e.g.*, Squirrel, Band-pass, and Band-rejection, the low- and high-frequency highly depend on the medium-frequency, and the medium-frequency is just the opposite. (2) The more difficult the task, the less obvious the dependency. In this task of Comb and ZINC, the dependency of eigenvalues is inconspicuous. This motivates us to consider more information to mine the dependency of challenging graphs. (3) In graph-level datasets, the decoder can learn different filters. Figure 5 shows two basic filters. It can be seen that $\hat{\boldsymbol{S}}_1$ and $\hat{\boldsymbol{S}}_2$ have different dependencies and shapes, which are different from node-level tasks, where only one filter is needed. This finding shows that graph-level tasks are more difficult than node-level tasks and are still challenging for spectral GNNs.

6 Conclusion

In this paper, we propose Specformer that leverages Transformer to build a set-to-set spectral filter along with learnable bases. Specformer effectively captures magnitudes and relative dependencies of the eigenvalues in a permutation-equivariant fashion and can perform non-local graph convolution. Experiments on synthetic and real-world datasets demonstrate that Specformer outperforms various GNNs and learns meaningful spectrum patterns. A promising future direction is to improve the efficiency of Specformer through sparsifying the self-attention matrix of Transformer.

REFERENCES

Muhammet Balcilar, Guillaume Renton, Pierre Héroux, Benoit Gaüzère, Sébastien Adam, and Paul Honeine. Analyzing the expressive power of graph neural networks in a spectral perspective. In *ICLR*, 2021.

Peter W Battaglia, Jessica B Hamrick, Victor Bapst, Alvaro Sanchez-Gonzalez, Vinicius Zambaldi, Mateusz Malinowski, Andrea Tacchetti, David Raposo, Adam Santoro, Ryan Faulkner, et al. Relational inductive biases, deep learning, and graph networks. *arXiv preprint arXiv:1806.01261*, 2018.

Deyu Bo, Xiao Wang, Chuan Shi, and Huawei Shen. Beyond low-frequency information in graph convolutional networks. In *AAAI*, pp. 3950–3957. AAAI Press, 2021.

Joan Bruna, Wojciech Zaremba, Arthur Szlam, and Yann LeCun. Spectral networks and locally connected networks on graphs. *arXiv preprint arXiv:1312.6203*, 2013.

Heng Chang, Yu Rong, Tingyang Xu, Yatao Bian, Shiji Zhou, Xin Wang, Junzhou Huang, and Wenwu Zhu. Not all low-pass filters are robust in graph convolutional networks. In *NeurIPS*, pp. 25058–25071, 2021.

Eli Chien, Jianhao Peng, Pan Li, and Olgica Milenkovic. Adaptive universal generalized pagerank graph neural network. In *ICLR*, 2021.

Michaël Defferrard, Xavier Bresson, and Pierre Vandergheynst. Convolutional neural networks on graphs with fast localized spectral filtering. In *NeurIPS*, pp. 3837–3845, 2016.

Jacob Devlin, Ming-Wei Chang, Kenton Lee, and Kristina Toutanova. BERT: pre-training of deep bidirectional transformers for language understanding. In *NAACL-HLT*, pp. 4171–4186. Association for Computational Linguistics, 2019.

Xiaowen Dong, Dorina Thanou, Laura Toni, Michael M. Bronstein, and Pascal Frossard. Graph signal processing for machine learning: A review and new perspectives. *IEEE Signal Process. Mag.*, 37(6):117–127, 2020.

Alexey Dosovitskiy, Lucas Beyer, Alexander Kolesnikov, Dirk Weissenborn, Xiaohua Zhai, Thomas Unterthiner, Mostafa Dehghani, Matthias Minderer, Georg Heigold, Sylvain Gelly, Jakob Uszkoreit, and Neil Houlsby. An image is worth 16x16 words: Transformers for image recognition at scale. In *ICLR*, 2021.

Vijay Prakash Dwivedi and Xavier Bresson. A generalization of transformer networks to graphs. *CoRR*, abs/2012.09699, 2020.

Vijay Prakash Dwivedi, Chaitanya K. Joshi, Thomas Laurent, Yoshua Bengio, and Xavier Bresson. Benchmarking graph neural networks. *CoRR*, abs/2003.00982, 2020.

Joan Bruna Estrach, Wojciech Zaremba, Arthur Szlam, and Yann LeCun. Spectral networks and deep locally connected networks on graphs. In *ICLR*, 2014.

Justin Gilmer, Samuel S Schoenholz, Patrick F Riley, Oriol Vinyals, and George E Dahl. Neural message passing for quantum chemistry. In *International conference on machine learning*, pp. 1263–1272. PMLR, 2017.

David K Hammond, Pierre Vandergheynst, and Rémi Gribonval. Wavelets on graphs via spectral graph theory. *Applied and Computational Harmonic Analysis*, 30(2):129–150, 2011.

Mingguo He, Zhewei Wei, Zengfeng Huang, and Hongteng Xu. Bernnet: Learning arbitrary graph spectral filters via bernstein approximation. In *NeurIPS*, 2021.

Mingguo He, Zhewei Wei, and Ji-Rong Wen. Convolutional neural networks on graphs with chebyshev approximation, revisited. In *NeurIPS*, 2022.

Weihua Hu, Matthias Fey, Marinka Zitnik, Yuxiao Dong, Hongyu Ren, Bowen Liu, Michele Catasta, and Jure Leskovec. Open graph benchmark: Datasets for machine learning on graphs. In *NeurIPS*, 2020.

Thomas N. Kipf and Max Welling. Semi-supervised classification with graph convolutional networks. In *ICLR*, 2017.

Devin Kreuzer, Dominique Beaini, William L. Hamilton, Vincent Létourneau, and Prudencio Tossou. Rethinking graph transformers with spectral attention. In *NeurIPS*, 2021.

Renjie Liao, Zhizhen Zhao, Raquel Urtasun, and Richard S. Zemel. Lanczosnet: Multi-scale deep graph convolutional networks. In *ICLR*, 2019.

Kenta Oono and Taiji Suzuki. Graph neural networks exponentially lose expressive power for node classification. In *ICLR*. OpenReview.net, 2020.

Antonio Ortega, Pascal Frossard, Jelena Kovacevic, José M. F. Moura, and Pierre Vandergheynst. Graph signal processing: Overview, challenges, and applications. *Proc. IEEE*, 106(5):808–828, 2018.

Ladislav Rampásek, Mikhail Galkin, Vijay Prakash Dwivedi, Anh Tuan Luu, Guy Wolf, and Dominique Beaini. Recipe for a general, powerful, scalable graph transformer. *CoRR*, abs/2205.12454, 2022.

Franco Scarselli, Marco Gori, Ah Chung Tsoi, Markus Hagenbuchner, and Gabriele Monfardini. The graph neural network model. *IEEE transactions on neural networks*, 20(1):61–80, 2008.

Han Shi, Jiahui Gao, Hang Xu, Xiaodan Liang, Zhenguo Li, Lingpeng Kong, Stephen M. S. Lee, and James T. Kwok. Revisiting over-smoothing in BERT from the perspective of graph. *CoRR*, abs/2202.08625, 2022.

Jake Topping, Francesco Di Giovanni, Benjamin Paul Chamberlain, Xiaowen Dong, and Michael M. Bronstein. Understanding over-squashing and bottlenecks on graphs via curvature. In *ICLR*. OpenReview.net, 2022.

Ashish Vaswani, Noam Shazeer, Niki Parmar, Jakob Uszkoreit, Llion Jones, Aidan N. Gomez, Lukasz Kaiser, and Illia Polosukhin. Attention is all you need. In *NeurIPS*, pp. 5998–6008, 2017a.

Ashish Vaswani, Noam Shazeer, Niki Parmar, Jakob Uszkoreit, Llion Jones, Aidan N Gomez, Łukasz Kaiser, and Illia Polosukhin. Attention is all you need. *Advances in neural information processing systems*, 30, 2017b.

Petar Velickovic, Guillem Cucurull, Arantxa Casanova, Adriana Romero, Pietro Liò, and Yoshua Bengio. Graph attention networks. In *ICLR*, 2018.

Peihao Wang, Wenqing Zheng, Tianlong Chen, and Zhangyang Wang. Anti-oversmoothing in deep vision transformers via the fourier domain analysis: From theory to practice. *CoRR*, abs/2203.05962, 2022.

Xiyuan Wang and Muhan Zhang. How powerful are spectral graph neural networks. In *ICML*, volume 162 of *Proceedings of Machine Learning Research*, pp. 23341–23362. PMLR, 2022.

Felix Wu, Amauri H. Souza Jr., Tianyi Zhang, Christopher Fifty, Tao Yu, and Kilian Q. Weinberger. Simplifying graph convolutional networks. In *ICML*, volume 97 of *Proceedings of Machine Learning Research*, pp. 6861–6871. PMLR, 2019.

Zonghan Wu, Shirui Pan, Fengwen Chen, Guodong Long, Chengqi Zhang, and Philip S. Yu. A comprehensive survey on graph neural networks. *IEEE Trans. Neural Networks Learn. Syst.*, 32 (1):4–24, 2021.

Bingbing Xu, Huawei Shen, Qi Cao, Yunqi Qiu, and Xueqi Cheng. Graph wavelet neural network. *arXiv preprint arXiv:1904.07785*, 2019.

Mingqi Yang, Yanming Shen, Rui Li, Heng Qi, Qiang Zhang, and Baocai Yin. A new perspective on the effects of spectrum in graph neural networks. In *ICML*, volume 162 of *Proceedings of Machine Learning Research*, pp. 25261–25279. PMLR, 2022.

Chengxuan Ying, Tianle Cai, Shengjie Luo, Shuxin Zheng, Guolin Ke, Di He, Yanming Shen, and Tie-Yan Liu. Do transformers really perform bad for graph representation? In *NeurIPS*, 2022.

Jie Zhou, Ganqu Cui, Shengding Hu, Zhengyan Zhang, Cheng Yang, Zhiyuan Liu, Lifeng Wang, Changcheng Li, and Maosong Sun. Graph neural networks: A review of methods and applications. *AI Open*, 1:57–81, 2020.

Meiqi Zhu, Xiao Wang, Chuan Shi, Houye Ji, and Peng Cui. Interpreting and unifying graph neural networks with an optimization framework. In *WWW*, pp. 1215–1226. ACM / IW3C2, 2021.

A EXPERIMENTAL DETAILS

A.1 DATASETS

Table 5: Detailed information of graph-level datasets.

	Graphs	**Avg. nodes**	**Avg. edges**	**Tasks**	**Metric**
ZINC	12,000	23.2	24.9	Regression	MAE
MolHIV	41,127	25.5	27.5	Binary Classification	AUROC
MolPCBA	437,929	26.0	28.1	128-task Classification	Average Precision

A.2 HYPERPARAMETERS

Table 6: Hyperparameters of node-level datasets.

Hyperparameter	**Synthetic**	**Chameleon**	**Squirrel**	**Actor**	**Cora**	**Citeseer**	**Photo**
Layer	1	2	2	2	2	2	2
Heads	1	4	2	1	2	2	4
Hidden dim	16	32	32	32	32	32	32
Epoch	2000	2000	2000	2000	2000	2000	2000
Learning rate	0.01	1e-3	1e-3	2e-4	2e-4	2e-4	2e-4
Weight decay	0	5e-4	1e-3	1e-4	1e-4	1e-3	1e-4
Transformer dropout	0	0.2	0.1	0.5	0.2	0	0.2
Feature dropout	0	0.4	0.4	0.8	0.6	0.7	0.3
Propagation dropout	0	0.5	0.4	0.5	0.2	0.5	0.2
Combination	Small	Medium	Medium	Medium	Medium	Medium	Medium
Parameters	2,084	82,445	74,787	37,680	53,885	126,840	32,044

Table 7: Hyperparameters of graph-level datasets.

Hyperparameter	ZINC	MolHIV	MolPCBA
Layer	4	8	8
Heads	8	4	8
Hidden dim	160	80	256
Graph pooling	mean	mean	mean
Epoch	1000	50	30
Warmup	50	5	5
Batch size	32	64	64
Learning rate	1e-3	1e-4	5e-4
Weight decay	5e-4	1e-4	5e-3
Transformer dropout	0.1	0.1	0.3
Feature dropout	0.05	0.1	0.1
Propagation dropout	0	0.3	0.1
Combination	Small	Medium	Large
Parameter	529,609	226,645	3,025,048

B IMPLEMENTATION DETAILS

B.1 SPECFORMER LAYER

Here we explain how to incorporate the Specformer layer with edge features. Specifically, we first broadcast the node features to the edges and filter the mixed edge features. Finally, the filtered edge

features are aggregated to yield new node features.

$$\begin{aligned} \boldsymbol{E} &= \boldsymbol{H}.\text{unsqueeze}(0) + \boldsymbol{E}, \\ \hat{\boldsymbol{E}} &= \boldsymbol{S} \odot \boldsymbol{E}, \\ \hat{\boldsymbol{H}} &= \hat{\boldsymbol{E}}.\text{sum}(0), \end{aligned} \tag{7}$$

where $\boldsymbol{H} \in \mathbb{R}^{N \times d}$ is the node feature matrix and $\boldsymbol{E} \in \mathbb{R}^{N \times N \times d}$ is the edge feature matrix.

B.2 Condensation of self-attention

In this section, we explain the details of the condensation of self-attention. We use $\boldsymbol{B}$ and $\hat{\boldsymbol{B}}$ to represent the self-attention matrix and its condensation.

$$\begin{aligned} \boldsymbol{B} &= \text{Softmax}(\frac{\boldsymbol{Q}\boldsymbol{K}^\top}{\sqrt{d_q}})\boldsymbol{V}, \\ \hat{\boldsymbol{B}} &= \text{Condense}(\boldsymbol{B}). \end{aligned} \tag{8}$$

Since $\boldsymbol{B}$ is row-normalized, we hope the condensation $\hat{\boldsymbol{B}}$ is still approximately row-normalized. For this purpose, we first sum the columns of $\boldsymbol{B}$ through the pre-defined frequency bands, e.g., Low, Medium, and High, and then average the rows.

$$\hat{\boldsymbol{B}}_{i,j} = \sum_{\lambda_p \in f_i} \sum_{\lambda_q \in f_j} \boldsymbol{B}_{p,q} \Big/ |\mathbf{1}_{\lambda \in f_i}|, \tag{9}$$

where f_i and f_j are the frequency bands, and $|\mathbf{1}_{\lambda \in f_i}|$ indicates the number of eigenvalues belonging to the frequency band f_i.

Through this condensation strategy, we can approximately preserve the self-attention matrix's information and find the frequency bands' dependency patterns.

C More experimental results

C.1 Eigenvalue encoding

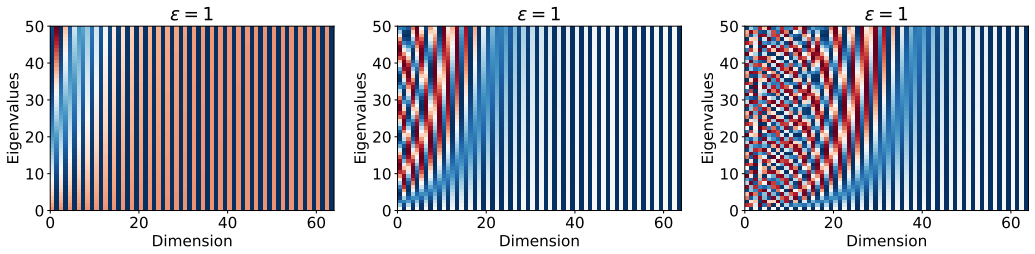

(a) $\epsilon = 1$ (b) $\epsilon = 10$ (c) $\epsilon = 100$

Figure 6: Eigenvalue encoding with different values of ϵ.

Here we visualize the outputs of eigenvalue encoding with different values of ϵ. Specifically, we uniformly sample 50 eigenvalues from the region $[0, 2]$ and map them into representations with $d = 64$. The results are shown in Figure 6. We can find that when $\epsilon = 1$, only the first 20 dimensions can distinguish different eigenvalues. As ϵ increases, the resolution of eigenvalue encoding becomes higher.